Archives of Photogrammetry, Cartography and Remote Sensing, Vol. 22, 2011, pp. 187-200
ISSN 2083-2214

MODEL-BASED AUTOMATIC 3D BUILDING MODEL GENERATION BY INTEGRATING LIDAR AND AERIAL IMAGES

Ayman Habib [1], Eunju Kwak [2], Mohannad Al-Durgham [3]

[1, 2] Department of Geomatics Engineering, University of Calgary, 2500 University Drive, Calgary, T2N 1N4, AB, Canada; (ahabib, ekwak)@ucalgary.ca
[3] Department of Civil Engineering, University of Toronto, 35 St. George Street, Toronto, M5S 1A4, ON, Canada; mohannad.al.durgham@utoronto.ca

KEY WORDS: LiDAR, Photogrammetry, Digital Building Model, Reconstruction

ABSTRACT: Accurate, detailed, and up-to-date 3D building models are important for several applications such as telecommunication network planning, urban planning, and military simulation. Existing building reconstruction approaches can be classified according to the data sources they use (i.e., single versus multi-sensor approaches), the processing strategy (i.e., data-driven, model-driven, or hybrid), or the amount of user interaction (i.e., manual, semiautomatic, or fully automated). While it is obvious that 3D building models are important components for many applications, they still lack the economical and automatic techniques for their generation while taking advantage of the available multi-sensory data and combining processing strategies. In this research, an automatic methodology for building modelling by integrating multiple images and LiDAR data is proposed. The objective of this research work is to establish a framework for automatic building generation by integrating data-driven and model-driven approaches while combining the advantages of image and LiDAR datasets.

1. INTRODUCTION

Accurate, detailed, and up-to-date 3D topographic information, including building models, are quite valuable for several applications. Natural disasters aftermath evaluation, search and rescue, urban planning, environmental studies, and military simulation are just examples where accurate digital building models are useful. With more accessible location-based services and personal navigation to the general public, the need for automated, realistic, and efficiently generated 3D models has become more urgent than ever (Brenner, 2005). Considering that the United Nations reported that more than 60% of the global population by 2030 will dwell in urban areas, up-to-date accurate 3D city models are required to properly plan for and accommodate this urban growth (UN-HABITAT, 2006). While it is obvious that 3D building models are important components, they still lack the economic and reliable techniques for their generation while taking advantage of the available multi-sensory data from single and multiple platforms.

Existing building reconstruction approaches can be classified according to the data sources they use (single versus multi-source approaches), the processing strategy (data-driven, model-driven, or hybrid) and the amount of user interaction (manual, semiautomatic, or fully automated) (Vosselman and Mass, 2010). Many research efforts have been conducted on building extraction over the last 20 years aiming at reducing the cost of producing models with a reasonable level of detail.

In terms of data source, aerial imagery has been and still is one of the common sources to obtain 3D building models based on traditional photogrammetric approaches. Despite the significant research efforts in the past, the low degree of automation remains as the major problem (Brenner, 2005). Thus, most of the current techniques have mainly relied on semi-automatic systems, in which recognition and interpretation tasks are performed by an operator, whereas modelling and precise measurement are supported through automation. Meanwhile, Light Detection And Ranging (LiDAR) has emerged as an important source of data for the generation of 3D city models due to the direct acquisition of reliable and dense 3D point cloud. While LiDAR has a great advantage of direct acquisition of three dimensional coordinates of points (thus, eliminating the need for the matching procedure), the positional nature of LiDAR data collection makes it difficult to derive semantic information from the captured surfaces. Moreover, the quality of the derived boundaries is inversely proportional to the point density. The integration of LiDAR data and aerial imagery provides more accurate solutions by combining the accurate height measurements of laser scanner and the planimetric accuracy of aerial images (Awrangjeb et al. 2010). The integration preserves the advantages of both datasets such as high-resolution texture and colour information from images together with intensity, height information, and potential higher automation from LiDAR data. Due to these advantages of integration, several researchers suggested integrating LiDAR and imagery for building detection (Cheng et al., 2008; Demir et al., 2009; Habib et al., 2010b to mention few).

In this research, an automatic methodology for building extraction and modelling by integrating multiple images and LiDAR data is proposed. In the following section, the detailed explanation of the proposed methodology is presented. In section 3 and 4, preliminary results and concluding remarks are mentioned, respectively.

2. METHODOLOGY

The reconstruction of the buildings can be carried out using three different approaches: Data-driven method (bottom-up), model-driven method (top-down) or hybrid method (Faig and Widmer, 2000; and Vosselman and Maas, 2010). The differences between the three approaches are manifested on how much relevant information regarding buildings is implemented during each process.

Data-driven approaches do not make assumptions regarding the building shapes in most cases using generic models. It has an advantage that it can model any shape of buildings, but at the same time the little knowledge of the models makes its implementation complex. Therefore, it leaves the question of how constraints and sets of rules should be imposed such as rectangularity, parallelism, etc (Brenner, 2005). Model-based approach uses parametric building models which are used as a hypothesis and verifies the model using information derived from the existing data. It predefines different basic building models in a database and the best fit model to the data is selected. Model-based methods are mostly implemented in a semi-automatic manner and use information from images. While the model-image fitting is solved automatically, the selection of a target model and an initial alignment of the model to the image are carried out manually by an operator (Tseng and Wang, 2003; Suveg and Vosselman, 2004).

The objective of this research work is to establish a framework for automatic building model generation by integrating data-driven and model-driven method while combining the advantages of image and LiDAR datasets. The proposed methodology can construct complex structures, which are comprised of a collection of rectangular primitives; however, this paper focuses on proposing a framework for automatic building model generation. Therefore, the whole process will be investigated using simple rectangular primitive. The developed procedures are comprised of three stages: 1) Pre-requsites, 2) Building segmentation and boundary generation from LiDAR data through a data-driven approach, and 3) Model-based image fitting of rectangular primitives. Fig. 1 illustrates the procedures in the proposed framework in this research. The following sections 2.1, 2.2, and 2.3 will give more details about the three procedures.

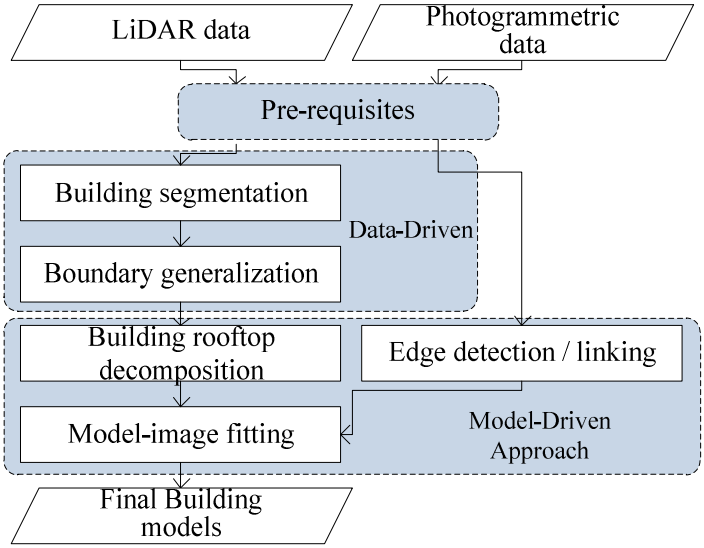

Fig. 1.The proposed framework for automatic building generation

2.1 Pre-requisites

To make use of the synergetic properties of combined photogrammetric and LiDAR data, the following prerequisite processes should be performed which are Quality Assurance (QA) of photogrammetric and LiDAR data, Quality Control (QC) of photogrammetric and LiDAR data, and co-registration of both dataset. The key activity in QA is the calibration procedure. To achieve the desired quality of final products, all the individual system components should be accurately calibrated and also the relationship between the various system components should be accurately estimated. For the photogrammetric system, Interior Orientation Parameters (IOP) is determined through a camera calibration process and spatial and rotational offsets between various system components (e.g., camera, GNSS and INS) are derived through total system calibration. A typical LiDAR acquisition system is composed of Global Positioning System (GPS), Inertial Navigation System (INS), and

laser scanning system. The calibration of a LiDAR system aims at the estimation of systematic errors in the system parameters (e.g., bore-sighting parameters). In this research, the camera and LiDAR systems are calibrated by adopting the approaches in Habib et al. (2006) and Habib et al. (2010a), respectively. QC is a post-mission procedure to verify whether the desired quality (i.e., data integrity, correctness, and completeness) has been achieved. This research adopts the QC method suggested by Habib et al. (2010a). This method utilizes linear features and patches extracted in a semi-automatic way and is based on the assumption that conjugate features from different strips should be collinear and coplanar in the absence of biases. Once the QA and QC of photogrammetric and LiDAR data verify the quality of the datasets, the data can be used with confidence. Since two datasets from different sources are utilized, they must be registered to a common reference frame. Photogrammetric geo-referencing is the process of defining the camera's position and attitude relative to the object space coordinate system at the moment of exposure. LiDAR data can be utilized as a source of control for photogrammetric geo-referencing. In previous work (Habib et al., 2008), we confirmed the feasibility of using the linear and areal features derived from LiDAR data as a source of control for photogrammetric geo-referencing. Therefore, in this research, the photogrammetric geo-referencing method proposed in Habib et al. (2008), is used. Straight-lines and planar patches are extracted from LiDAR data in a semi-automatic way and used as the registration primitives for photogrammetric and LiDAR dataset registration. Point-based bundle adjustment processes with modified weight matrices are used to incorporate linear and planar features (Habib et al., 2010a).

2.2 Model primitive generation: Data-Driven approach

This section discusses data-driven procedures to generate initial building model primitives (i.e., rectangular boundaries) from LiDAR dataset, which later will be used as an input model during the model-based image fitting process. The model primitive generation starts with hypothesizing potential buildings by differentiating buildings from other objects in the original LiDAR point clouds. A fully automated region grouping and merging segmentation algorithm has been developed for the processing of LiDAR data. The boundary of the plane segmentation results are traced and regularised to identify rectangles that best represent rooftop of the buildings.

2.2.1.Building segmentation:

Building segmentation focuses on the extraction of planar rooftops from LiDAR data. The utilized algorithm employs a sequential least squares plane fitting for optimal performance. We randomly select 5% of the LiDAR point cloud as seed points for the region growing process. For each seed point, n-neighboring points will be used for the initial plane fitting. If the standard deviation of the fitted plane is less than LiDAR-reported point Root Mean Square (RMS) error, the region growing starts. A normal distance to the plane from neighboring n points for every point in the group is checked and using accepted points, the plane parameters are updated after every point is accepted. This process is repeated until no more points are added to the plane. The group of planar patches containing the largest number of neighboring planes is considered as ground, and the rest is considered as building features which will be utilized for our research.

2.2.2.Boundary generalisation:

As a result of the segmentation process, planar patches constituting rooftops are derived and plane parameters (a, b, c, where, $Z = aX + bY + c$) of each plane are stored for the model-based image fitting procedure. To obtain the boundary of the identified planes, a modified convex hull method is applied on the segmented planes (Sampath and Shan, 2007). It should be noted that the derived boundaries from the segmented planes do not represent the actual boundaries of the physical objects due to the relatively low sampling rate of airborne LiDAR systems. To present the actual shape of the boundaries, the traced boundary from LiDAR should be regularized. Considering the target building shape of this research (i.e., building composed of sets of rectangles), it can be regularized as several rectangles that represent the rooftop of the building boundaries. For this purpose, the Minimum Bounding Rectangle (MBR) algorithm is introduced (Freeman and Shapira, 1975; Chaudhuri and Samal, 2007). The MBR derived rectangle is represented by the minimum and maximum coordinate values for the boundary points in 2D. It is determined by choosing the minimum area rectangle among the rectangles with an arbitrary orientation that contains the vertices of boundaries. Fig. 2 presents aerial image of a rectangular building (a), its segmentation result (b) and its initial boundary (c). As seen in Fig. 2 (d), traced boundary of a simple rectangle building from LiDAR segmentation is regularized as a rectangle which contains all the vertices of boundaries.

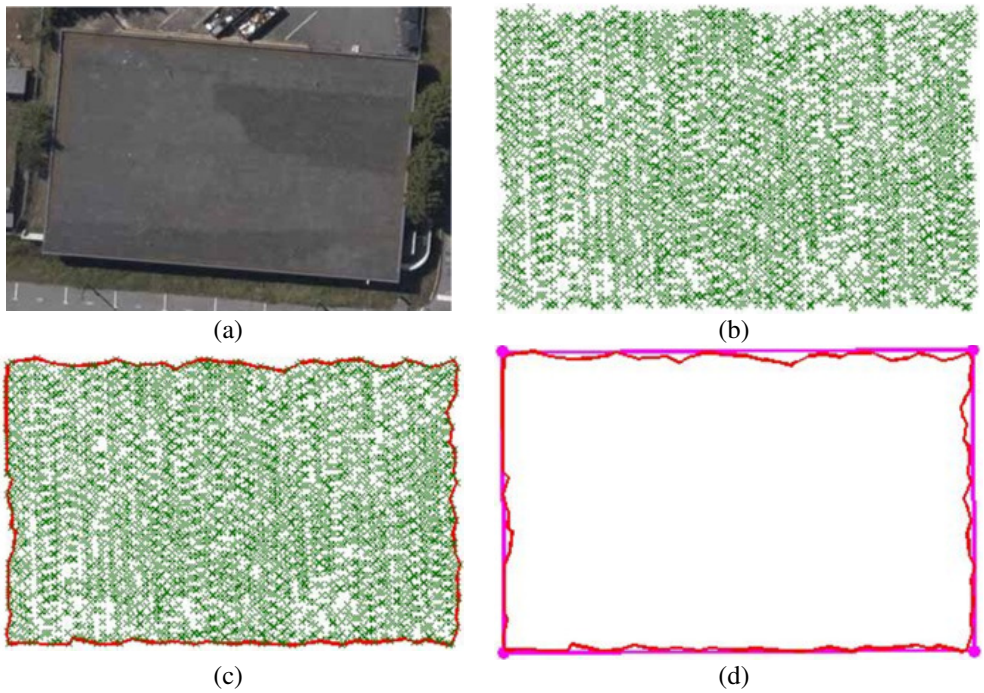

Fig. 2. aerial image (a), segmented LiDAR patch (b), traced boundary (c), and regularized boundary (d).

2.3 Model-based image fitting: Model-based approach

From the previous data-driven building detection procedure using LiDAR data, the initial model primitives are derived. This model will be adjusted to improve the horizontal accuracy while keeping the high LiDAR vertical accuracy by integrating image information. Although image-based boundary detection algorithms give higher quality, the matching ambiguities in multiple images remain as the main obstacle. In this regard, the rectangular model primitives defined from LiDAR data are incorporated to restrict the search space and resolve the matching ambiguities in multiple images. The parameters that define the models are adjusted using detected edges in the imagery by minimizing the normal distance between the detected edges and the projected ones through least-squares adjustment procedure that can simultaneously handle several images.

2.3.1. Building modelling and parameter estimation:

According to the constructive solid geometry (CSG) principle, each primitive should be associated with some parameters to adjust its geometric properties. These parameters are categorized into pose and shape parameters. Pose parameters define the position and orientation of the model primitives in object space using 3 translation parameters (X_0, Y_0, Z_0) and 3 rotation parameters (ω, φ, κ) as seen in Fig. 14. Previous literatures (Tseng and Wang, 2003; Suveg and Vosselman, 2004) suggest, since buildings stand vertical with horizontal rooftop, ω, φ are not considered and only use a rotation angle around Z-axis (κ). For more general building models (i.e., not only horizontal rooftops), ω, φ angles can be calculated using the orientation of the normal to the planar surface as defined by LiDAR segmentation.

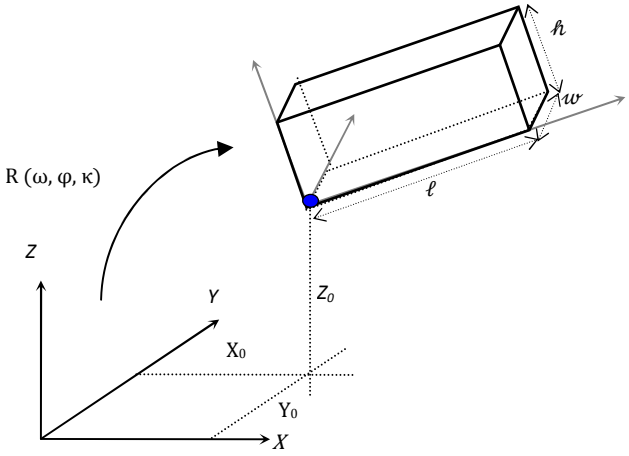

Fig. 14. Definition of pose and shape parameters

The shape parameters are associated with shape and size of the model; therefore, different models will be represented using different shape parameters (Tseng and Wang, 2003). Solid

box primitive, the most popular basic model primitive, is able to represent a building with the shape parameters of length (ℓ), width (w) and height (h). However, in the imagery, there is no guarantee that both roof top and bottom of the building are shown all the time, so h is hard to be determined from imagery only. In addition, it is known that the vertical position accuracy of LiDAR data is higher than the horizontal one, which suggests that the elevation of the building roof patch generated from LiDAR data is more reliable than the derived boundaries themselves. Therefore, in this research, h is determined using LiDAR data. By utilizing rectangular primitive, complex buildings that are comprised of rectangles and gable-roofs can be reconstructed. Therefore, in this research, the related parameters that define the rectangular primitives are reduced into 3 pose parameters (X_0, Y_0, κ) and 2 shape parameters (ℓ and w). These five parameters would be refined through the image-model fitting. One should note that we already have a good estimation of the initial values of the five parameters from LiDAR data. A rectangular primitive derived from LiDAR data is transformed into image coordinate system to integrate image information using already known EOPs and IOPs from Section 2.1.

2.3.2. Building rooftop decomposition:

As mentioned before, CSG can be used to construct complex building models by combining a set of basic primitives. In this work, automatic modelling of complex buildings using rectangular primitives is introduced. The question remaining is how to decompose complex structures into several basic primitives automatically. To decompose the initial model primitives into simple rectangular primitives, two conditions should be considered. First, the decomposition process should divide a regularized boundary into a collection of rectangles such that a portion or the entire length of the four sides for each rectangle must overlap with the physical building edges. This condition is necessary to have edge information from all sides in the images. Another consideration would be to minimize the number of involved model parameters for the image-fitting process as well as reducing the amount of needed post-processing (i.e., establishing the common reference point (X_0, Y_0) and orientation angle (κ)). The parameters of all the decomposed primitives would be adjusted simultaneously during the model-based image fitting process.

2.3.3. Edge detection and linking:

Fig. 4(a) depicts the projected rectangular model primitive under consideration into the imagery using the provided EOP, IOP and initial model parameters. The initial model parameters are acquired from LiDAR data segmentation and regularization, so the initial projection should be close to the actual outlines of the building roof on the aerial photo.

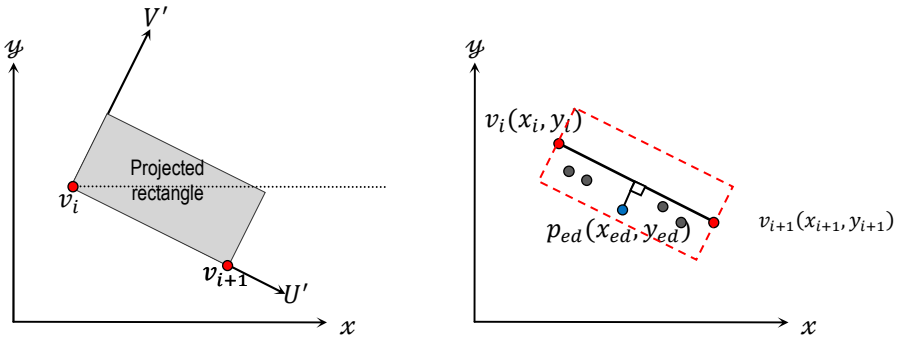

(a) (b)

Fig. 4. Projected rectangular model primitive onto the image space (a), and the effective buffer zone for one of the edges (b)

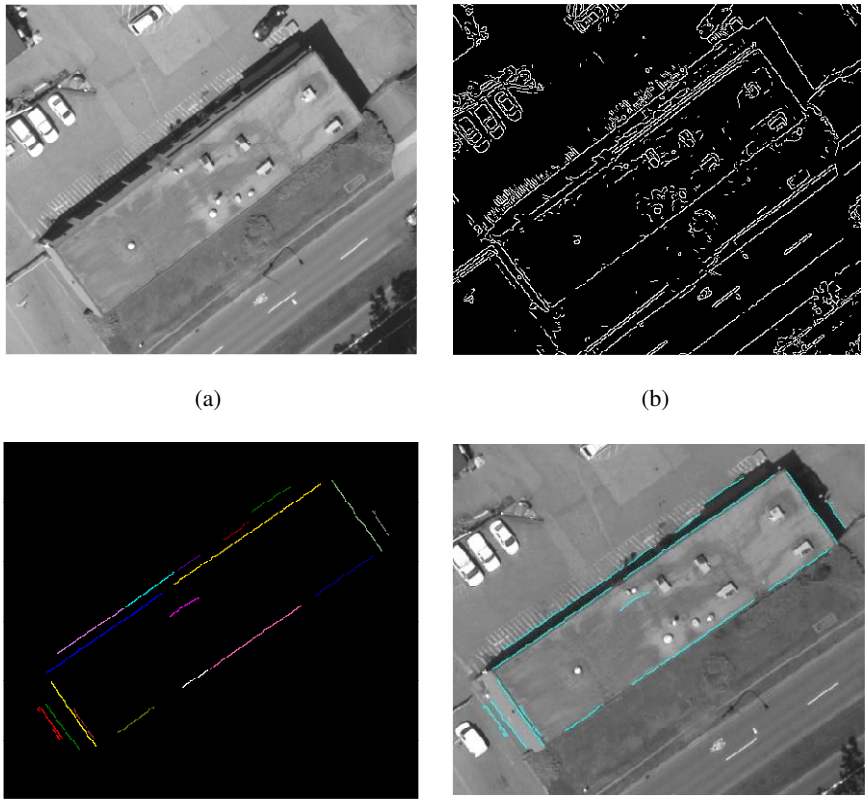

(a) (b)

(c) (d)

Fig. 5. aerial photo over the area of interest (a), canny edge detection (b),edge linking (different grouped lines are in different colours) (c), and extracted edges after filtering (d)

Based on the initial projection of the model onto the images, a buffer is set around each edge of the rectangle and only edge pixels within the buffer are utilized for the next step (Fig. 4(b)). All the extracted edges from images do not necessarily represent the rooftop boundaries due to occlusions, noise or irrelevant features near or on the roofs. Inadequate edge information may lead to the wrong solution for the model-image fitting. Therefore, selecting true edge information is important. Discrete edge points are first detected by applying the Canny edge detector (Canny, 1986) to the multiple images in which the building appears. Canny edge detector is one of the most common edge detection methods used in the image processing research which theoretically produces thin edges close to the true edges. However, as seen in Fig. 5(b) it produces unnecessary edges because of noise, non-uniform illuminations, and shadows. Therefore, the edge pixels that do not have similar direction to the LiDAR derived line are not considered by utilizing gradient angle information as it relates to the orientation of the projected boundaries. To remove unnecessary small segments, edge linking is performed on the edge pixels and segments whose length is smaller than a given threshold are removed. This process is applied to all the images where the building primitive appears in. Fig. 5(c) shows edge linking results where different colours represent different linked edge groups. The filtered edge pixels which exceed a predefined length and have similar direction to initial LiDAR lines within the buffer area are seen in Fig. 5(d). When compared with Fig. 5(b) (detected edges using canny operator), unnecessary edge information is removed.

2.3.4. Optimal model-image fitting:

The principle of model-image fitting is to adjust the unknown model parameters until the model fits to the edges extracted from the corresponding images. This is achieved by adding observation equations that minimize the normal distance between the detected edge pixels within the buffer and the projected line from LiDAR data while refining the model parameters. Each selected pixel p_{ed} contributes one set of observation equations assuming that one of the vertex points of the rectangle (v_i) and edge pixel (p_{ed}) are conjugate in Fig. 6. These points will be referred to as pseudo-conjugate points.

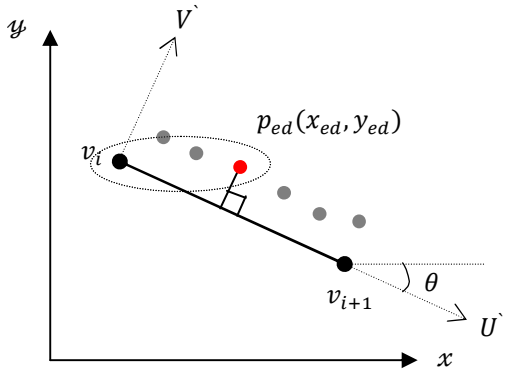

Fig. 6. Pseudo-point correspondence between the vertex of the rectangle and edge pixels

However, the vertex point (v_i) and the edge points(p_{ed}) are not corresponding to each other and have a discrepancy vector D between them. Additional unknown vector, D, is introduced by using non-conjugate points which are located along same lines. The mathematical model describing the discrepancy between pseudo conjugate points will take the form in Equation (1). The stochastic model describing the mathematical relationship among pseudo-conjugate points can be represented by the Gauss Markov Stochastic model in Equation (1).

$$y = Ax + D + e \quad e \sim (0, \Sigma) \quad where\ \Sigma = \sigma_o^2 P^{-1} \tag{1}$$

In order to use the model in Equation (1) while eliminating the unknown vector D from the parameters to be estimated, a modified least square adjustment procedure is developed (Habib et al. 2010a). The modification starts by changing the stochastic properties of the random noise vector as represented by Equation (2). The new weight matrix P' of the noise vector is chosen such that $P'D = 0$

$$\Sigma`\{e\} = \sigma_o^2\, P'^{+} \quad where \quad P'D = 0 \tag{2}$$

Therefore, the modified variance-covariance matrix will be represented as follows $\Sigma`\{e\} = \sigma_o^2\, P'^{+}$, where the plus sign indicates the Moore-Penrose pseudo inverse. Starting from the modified weight matrix, the LSA target function can be redefined as in Equation (3). Thus, the solution ($\hat{x}$) to the LSA target function is defined by Equation (4). Using the law of error propagation, the variance covariance matrix of the solution vector, $\Sigma\{\hat{x}\}$, is shown in Equation (5). Finally the a-posteriori variance factor($\hat{\sigma}_o^2$) is estimated according to Equation (6), where q is the rank of the modified weight matrix $P`$and m is the number of unknown (refer to Habib et al. 2010a for the detailed derivation).

$$\begin{aligned} e^T P` e &= (y - Ax - D)^T P` (y - Ax - D) \\ &= (y - Ax)^T P` (y - Ax) = min|_x \end{aligned} \tag{3}$$

$$\hat{x} = (A^T P` A)^{-1} A^T P` y = N^{-1} A^T P` y \tag{4}$$

$$\Sigma\{\hat{x}\} = \sigma_o^2 N^{-1} \tag{5}$$

$$\hat{\sigma}_o^2 = (y - A\hat{x})^T P` (y - A\hat{x})/(q - m) \tag{6}$$

Thus, the modification in the weights of the noise vector allows for the elimination of the additional unknown vector, D, while having almost no impact on the traditional LSA (i.e., the solution is obtained using the traditional solution for the Gauss Markov Model in the absence of the additional unknown vector D resulting from the use of pseudo-conjugate points along a corresponding point-line pair.

3. EXPERIMENTAL RESULTS

In this paper, fully-automatic 3D building model generation methodology is proposed by providing the initial rectangular model primitive from LiDAR data and adjusting the initial

model through model-based image fitting process. To test the validity of the proposed methodology, preliminary results using a rectangular building is presented in this section.

3.1 Dataset Description

The dataset used in the experiments is captured over the British Colombia Institute of Technology (BCIT) in Vancouver. The dataset includes multiple aerial images and airborne LiDAR data collected over the same area. A brief description of the dataset is given in Table 1.

Tab. 1. Dataset specifications

	Photogrammetric data	LiDAR data
System	MFDC Rollei P-65	Leica ALS50
Average flying height	540 and 1,150 m	540 and 1,150 m
GSD (image) Average point density (LiDAR)	5 and 10 cm	1.5 and 4.0 pts/m^2

3.2 Model-image fitting result

To test the model-based image fitting algorithm, a simple rectangular building that appears in 3 images is selected from the BCIT dataset. Fig. 7 shows an aerial image over the target building and initial traced boundary respectively.

Fig. 7. aerial image over area of interest (a), and initial LiDAR boundary (b)

Based on the result from Fig. 7(b), the MBR is derived and the initial parameters are acquired. Fig. 8 shows the projected MBR onto the images (in red) and the extracted edge pixels (in yellow) within the defined buffer from the three images. Note that we can use as many images as available. Even though the initial position derived from LiDAR data is quite close to the actual boundary, there are deviations in some edges which need improvement.

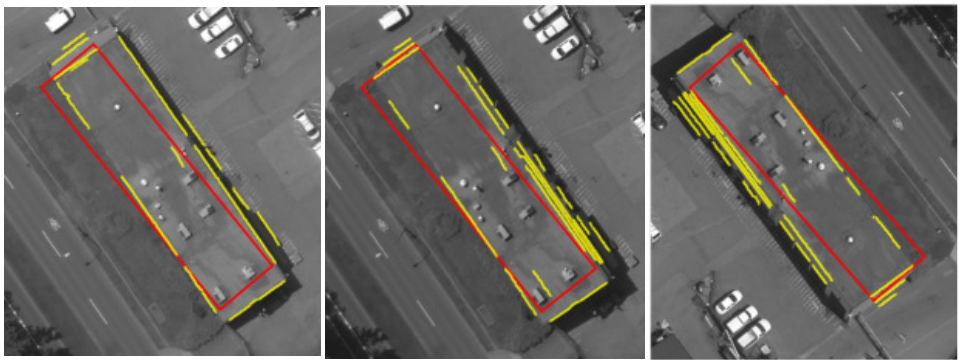

(a) (b) (c)

Fig. 8. Projection of the rectangular primitive using LiDAR-based initial parameters onto three images (a), (b), (c)

After the automatic model-image fitting procedure, the final adjusted rectangular primitive is projected onto the three images in Fig. 9.

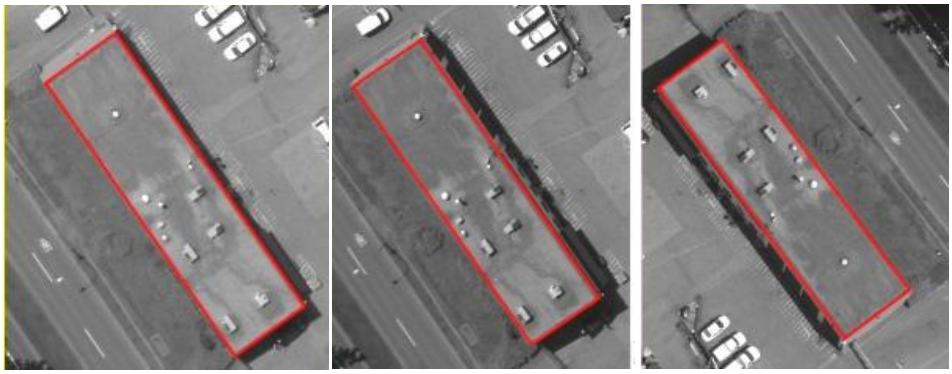

(a) (b) (c)

Fig. 9. Projection of the rectangular primitive after model-based image fitting onto three images (a), (b), (c)

When visually checked, the rectangular primitive is adjusted close to the extracted edge pixels from images. Although this algorithm can be applied using a single image, increasing number of images would provide different views of the same buildings, so the adjusted result will be more reliable and robust to potential occlusions. Table 2 presents the initial values of the pose/shape parameters, final adjusted values, and standard deviations from Equation (5). The standard deviations of adjusted parameters are all within acceptable range considering that GSD is 10cm. The standard deviation of ℓ value is slightly higher than other parameters, because the two images show the walls of the building along the ℓ sides which might include edge pixels from the side walls. The extracted edge pixels have a great effect on the accuracy of the final model primivites, therefore, additional algorithm for extracting only relavant edges need to be implemented.

Tab. 2. Original and estimated values for the unknown model parameters and their standard deviation

Unknown Parameter	Initial value from LiDAR data	Final value after adjustment	Standard deviation of adjusted parameters
X_0 (m)	500238	500239.626	0.008
Y_0 (m)	5455402	5455404.374	0.007
w (m)	10	11.571	0.007
ℓ (m)	42	43.823	0.012
κ (°)	-138	-142.133	0.008

4. CONCLUSIONS AND FUTURE WORK

The advantage of the proposed approach is that it can utilize any number of images and overcome the limitation of occlusions which are the most common problem when dealing with large scale imagery. The initial approximation values for the models are derived automatically from LiDAR data, which eliminates the need for human intervention as opposed to what is implemented in previous studies. Complex models can be partitioned into simple rectangular primitives automatically which will be addressed in future publications. The research will lead to a practical and economic platform for Geographic Information System (GIS) compilation and a reliable 3D model generation. While utilizing existing available data and minimizing the human interaction, which translates into reduced cost and the need for technical expertise, the proposed procedure maintains the quality of the end product.

ACKNOWLEDGEMENTS

This work was supported by the Canadian GEOIDE NCE Network (IV-17) and the National Science and Engineering Council of Canada (Discovery Grant). The authors would like to thank McElhanney Consulting Services Ltd, BC, Canada for providing the real dataset and technical feedback.

REFERENCES

Awrangjeb, M., Ravanbakhsh, M., and Fraser, C.S., 2010. Automatic detection of residential buildings using LiDAR data and multispectral imagery, *ISPRS Journal of Photogrammetry & Remote Sensing,* 65, pp. 457-467.

Brenner, C., 2005. Building reconstruction from images and laser scanning, *International Journal of Applied Earth Observation and Geoinformation*, Vol 6, Issues 3-4, pp. 187-198.

Canny, J., 1986. A computational approach to edge detection, *IEEE Transactions on Pattern Analysis and Machine Intelligence*, Vol 8, pp. 679–690.

Chaudhuri, D., and A. Samal, 2007. A simple method for fitting of bounding rectangle to closed regions, *Pattern Recognition*, 40, pp. 1981-1989.

Cheng, L., Gong, J., Chen, X., Han, P., 2008. Building boundary extraction from high resolution imagery and LIDAR data. *International Archives of the Photogrammetry, Remote Sensing and Spatial Information Sciences,* 37 (Part B3), pp. 693- 698

Demir, N., Poli, D., Baltsavias, E., 2009. Extraction of buildings using images & LIDAR data and a combination of various methods. *International Archives of the Photogrammetry, Remote Sensing and Spatial Information Sciences*, 38 (Part 3/W4), pp.71-76.

Faig, W., and T. Widmer, 2000. Automatic building extraction from aerial images, *Proc.Of IAPRS*, Vol.33, B7, pp.1708-1715, Amsterdam, Netherlands.

Freeman, H., and R.Shapira, 1975. Determining the minimum-area encasing rectangle for an arbitrary closed curve, *Communications of ACM*, Vol. 18, Num. 7.

Habib, A., Quackenbush, P., Lay, J., Wong, C., and Al-Durgham, M., 2006. Camera calibration and stability analysis of medium-format digital cameras. *Proceedings of SPIE* – 6312, Applications of Digital Image Processing XXIX, 11 pages.

Habib, A., Jarvis, A., Kersting, A., Alghamdi, Y., 2008. Comparative Analysis of Geo-referencing Procedures Using Various Sources of Control Data, *XXIst ISPRS proceedings*, 3-11 Jul, 2008, Beijing, China, 27: 1147 – 1152.

Habib A., K. I. Bang, A. P. Kersting, 2010a. Alternative Methodologies for LiDAR System Calibration, *Remote Sensing*, 2(3): 874-907.

Habib, A., R. Zhai, and C. Kim, 2010b. Generation of complex polyhedral building models by integrating stereo-aerial imagery and LiDAR data. *Photogrammetric Engineering and Remote Sensing*, Vol. 76, 609-623.

Sampath, A. and J. Shan, 2007. Building boundary tracing and regularization from airborne LiDAR point clouds, *Photogrammetric Engineering and Remote Sensing*, 73(7): 805-812.

Suveg, I., and Vosselman, G., 2004. Reconstruction of 3D building models from aerial images and maps. *ISPRS Journal of Photogrammetry and Remote Sensing*, 58, pp. 202–224.

Tseng, Y.H, and S. Wang, 2003. Semiautomated Building Extraction Based on CSG Model-Image Fitting, *Photogrammetric Engineering and Remote Sensing*, 69(2), pp. 171-180.

UN-HABITAT, 2006. State of the World's Cities, 2006/7.

Vosselman, G., and H.G. Maas., 2010. Airborne and Terrestrial Laser Scanning, Whittles Publishing, Scotland, UK.